Letters

Derivation of a Condition for the Normal Gain Behavior of Pyramidal Horns

Krishnasamy T. Selvan

***Abstract*—The pyramidal horn exhibits a normal monotonically increasing gain versus frequency characteristic, only when its axial length is more than a certain minimum value for given aperture dimensions. In this letter, approximate equations are derived for estimating this minimum axial length.**

***Index Terms*—Normal gain behavior, pyramidal horn gain, Schelkunoff's formula.**

I. Introduction

A monotonically increasing gain with the operating frequency has been considered to be a salient feature of aperture antennas [1] that include pyramidal horns. The practical usefulness of this feature, which is conditional upon the aperture efficiency remaining constant with frequency, is that it allows the designer to be confident of obtaining a certain minimum gain.

Optimum gain pyramidal horns [2], [3] exhibit such a "normal" gain versus frequency pattern, if the periodic variations in the gain curve [4], [5] are not considered. But what could be an explicit condition for nonoptimum, or short horns, to display this behavior? It is the intent of this letter to address this question.

Considering the geometry of the pyramidal horn shown in Fig. 1, the E- and H-plane phase errors in wavelengths are approximately given by

$$s = \frac{b_1^2}{8\lambda l_1} \qquad t = \frac{a_1^2}{8\lambda l_2} \tag{1}$$

where $l_1 = \sqrt{l_E^2 - b_1^2/4}$ and $l_2 = \sqrt{l_H^2 - a_1^2/4}$. Thus the phase error depends only on the axial length for a fixed aperture. Gain depends on phase error through the reduction factors R_E and R_H [6]; and, the larger the initial phase error, the more sensitive the gain becomes to further variations in it [7]. Therefore, it should be expected that if the initial phase error is more than a certain value, further increase in the error as frequency increases will so affect the gain as to decrease it with frequency. Thus, for a certain aperture, a minimum axial length is required for the pyramidal horn to preserve its "normal" gain behavior. We will now derive approximate expressions for determining this minimum axial length.

II. Approximation for Gain Reduction Factors

Schelkunoff's horn gain equation can be written as [8]

$$g(f) = 113.3 a_1 b_1 f^2 \left[10^{-(D_H + D_E)/10}\right] \tag{2}$$

where a_1 and b_1 are in m, and f is frequency in GHz. D_H and D_E are the H- and E-plane gain reduction factors in dB, with the following polynomial approximations [8]:

$$D_H = (0.01\alpha)(1 + 10.19\alpha + 0.51\alpha^2 - 0.097\alpha^3) \tag{3}$$

$$D_E = (0.1\beta^2)(2.31 + 0.053\beta) \tag{4}$$

where

$$\alpha = \frac{a_1^2 f}{0.3 l_2} \qquad \beta = \frac{b_1^2 f}{0.3 l_1}. \tag{5}$$

These polynomial approximations give a fairly accurate representation of the gain reduction factors for $0 < \alpha, \beta < 6$. This is fine in practical considerations as most horns have $0 < \alpha, \beta < 4$ [6]. It can be shown that further simplification of (3) by avoiding the fourth-degree term does not significantly affect its accuracy for $0 < \alpha < 6$. Therefore, we will use the following approximation for D_H in our further discussions:

$$D_H = (0.01\alpha)(1 + 10.19\alpha + 0.51\alpha^2). \tag{6}$$

III. Minimum Axial Length

The problem is to determine the minimum axial length L such that $g(f)$ remain a monotonically increasing function in the desired frequency range $f_1 \le f \le f_2$.

In terms of axial length L, α and β can be written as

$$\alpha = y\,\frac{f}{L} \qquad \beta = z\,\frac{f}{L} \tag{7}$$

where

$$y = \frac{a_1(a_1 - a)}{0.3} \qquad z = \frac{b_1(b_1 - b)}{0.3}. \tag{8}$$

By using (4), (6), and (7), (2) can be written as

$$g(f) = 113.3 a_1 b_1 f^2 \left\{10^{-[\alpha_1 (f/L) + \alpha_2 (f^2/L^2) + \alpha_3 (f^3/L^3)]}\right\} \tag{9}$$

where

$$\begin{aligned} \alpha_1 &= 0.001y \\ \alpha_2 &= 0.01019y^2 + 0.0231z^2 \\ \alpha_3 &= 0.00051y^3 + 0.00053z^3. \end{aligned} \tag{10}$$

In order to be a monotonically increasing function in the range $f_1 \le f \le f_2$, the derivative of $g(f)$ must be greater than zero in this range. In mathematical terms

$$\log_e 10\left(-3\alpha_3 \frac{f^3}{L^3} - 2\alpha_2 \frac{f^2}{L^2} - \alpha_1 \frac{f}{L}\right) + 2 > 0. \tag{11}$$

By introducing the new variable x, we now make the substitution $f = xL$ in (11). Then, dividing the resulting equation by $3\alpha_3$ and multiplying by -1, (11) becomes

$$x^3 + \frac{2\alpha_2}{3\alpha_3} x^2 + \frac{\alpha_1}{3\alpha_3} x - \frac{2}{3\alpha_3 \log_e 10} < 0. \tag{12}$$

Equation (12) has to be satisfied in order that $g(f)$ monotonically increases in the frequency band $f_1 \le f \le f_2$. Fig. 2 illustrates the typical

Manuscript received May 17, 1999; revised July 13, 2000.

The author is with SAMEER—Centre for Electromagnetics, CIT Campus, Taramani, Madras-600 113 India (e-mail: sameercem@vsnl.com).

Publisher Item Identifier S 0018-926X(00)10840-3.

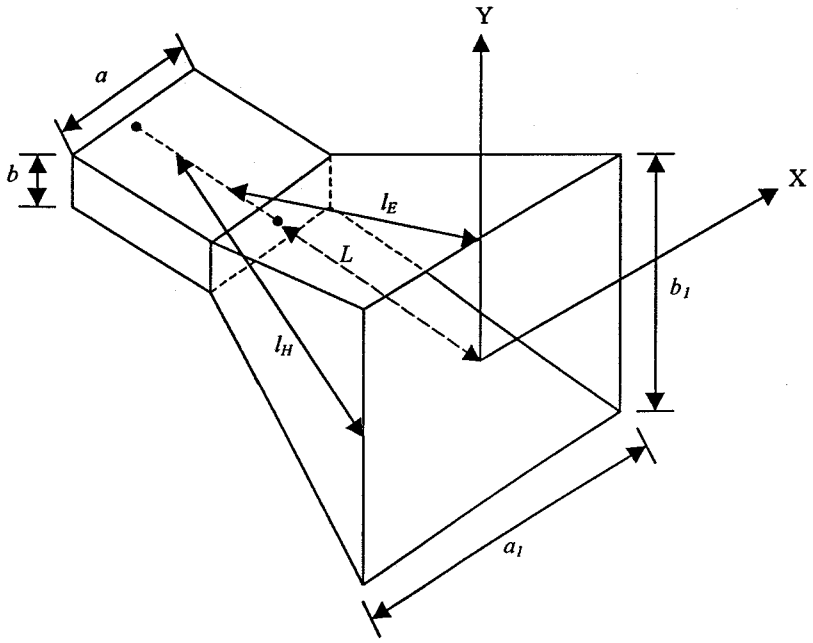

Fig. 1. Geometry of pyramidal horn.

behavior of the cubic equation (12). Thus, (12) has three real roots, of which only one is positive for physically realizable horns. This positive root x_1 of (12) is given by the following [9]:

$$x_1 = (s_1 + s_2) - \frac{c_2}{3} \tag{13}$$

where

$$s_1 = \left[p + \sqrt{q^3 + p^2}\right]^{1/3} \tag{14}$$

$$s_2 = \left[p - \sqrt{q^3 + p^2}\right]^{1/3} \tag{15}$$

$$c_2 = \frac{2\alpha_2}{3\alpha_3} \tag{16}$$

$$p = \frac{1}{6}\left[\frac{2\alpha_1\alpha_2}{9\alpha_3^2} + \frac{2}{\alpha_3 \log_e 10}\right] - \frac{1}{27}\left(\frac{2\alpha_2}{3\alpha_3}\right)^3 \tag{17}$$

$$q = \frac{1}{9}\left[\frac{\alpha_1}{\alpha_3} - \left(\frac{2\alpha_2}{3\alpha_3}\right)^2\right]. \tag{18}$$

It maybe noted that s_1 and s_2 form a complex conjugate pair.

If f_2 is the upper frequency, then we have, with reference to Fig. 2

$$L_{\min} = \frac{f_2}{x_1} \tag{19}$$

as the minimum axial length required for a horn with $0 < \alpha,\ \beta < 6$. It may be noted that this length will always be less than the "optimum" length, i.e., the length of a horn designed to offer optimum gain. Subject to the horn having a minimum axial length given by (19) for given aperture, it will display normal gain behavior in its frequency band.

For the case of a horn with the aperture dimensions $a_1 = 10.2$ cm, $b_1 = 8.3$ cm in the frequency range 18–26.5 GHz, (19) predicts a minimum axial length L of about 20 cm. If for example, an axial length of 16 cm is chosen instead, the gain starts falling at about 23.5 GHz, as shown in Fig. 3.

IV. Summary

Approximate expressions were derived for estimating the minimum axial length required by pyramidal horns with $0 < \alpha,\ \beta < 6$ to ex-

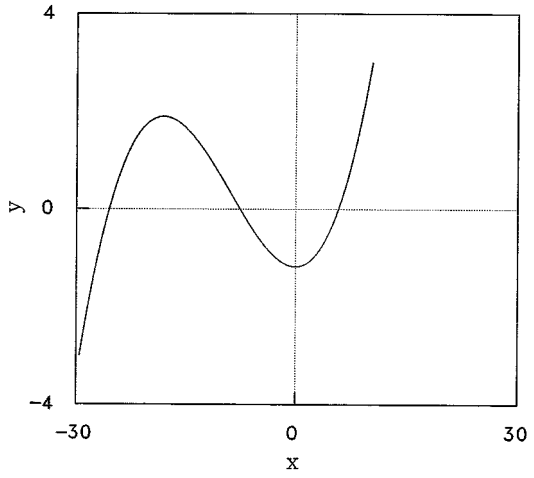

Fig. 2. Typical behavior of cubic equation (12) for pyramidal horn.

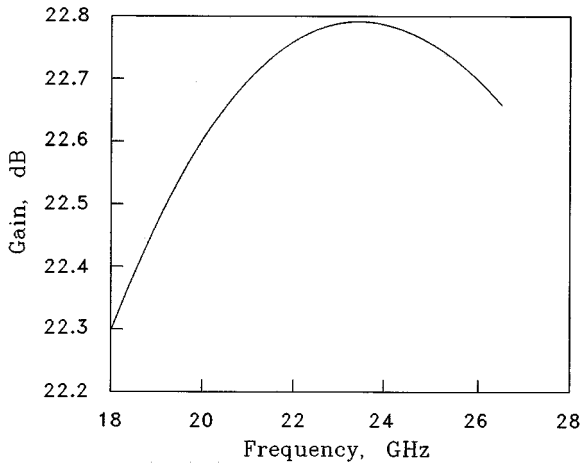

Fig. 3. Gain pattern for a K-band horn with less than minimum required axial length. The dimensions are $a = 1.1$ cm, $b = 0.43$ cm, $a_1 = 10.2$ cm, $b_1 = 8.3$ cm, $L = 16$ cm.

hibit normal monotonically increasing gain behavior. If more general formulas are desired for determining the minimum axial length, then the gain reduction factors must be employed without approximations. This would, of course, be possible but more involved.

ACKNOWLEDGMENT

The author would like to thank Dr. G. Date of The Institute of Mathematical Sciences, Madras, for useful discussions and the reviewers for constructive comments.

REFERENCES

[1] W. L. Stutzman and G. A. Thiele, *Antenna Theory and Design*. New York: Wiley, 1998.
[2] C. A. Balanis, *Antenna Theory Analysis and Design*. New York: Harper Row, 1982.
[3] K. T. Selvan, "Accurate design method for optimum gain pyramidal horns," *Electron. Lett.*, vol. 35, no. 4, pp. 249–250, Feb. 1999. [Corrections, *Electron. Lett.*, vol. 35, no. 7, p. 607, Apr. 1999].
[4] E. V. Jull, "Errors in the predicted gain of pyramidal horns," *IEEE Trans. Antennas Propagat.*, vol. AP-21, pp. 25–31, Jan. 1973.
[5] J. F. Nye and W. Liang, "Theory and measurement of the field of a pyramidal horn," *IEEE Trans. Antennas Propagat.*, vol. 44, pp. 1488–1498, Nov. 1996.
[6] E. V. Jull, "Finite-range gain of sectoral and pyramidal horns," *Electron. Lett.*, vol. 6, no. 21, pp. 680–681, Oct. 1970.
[7] E. H. Braun, "Gain of electromagnetic horns," *IRE Proc.*, vol. 41, pp. 109–115, Jan. 1953.
[8] M. Kanda and R. D. Orr, "Near-field gain of a horn and an open-ended waveguide: comparison between theory and experiment," *IEEE Trans. Antennas Propagat.*, vol. 35, pp. 33–40, Jan. 1987.
[9] M. Abramowitz and I. A. Stegun, Eds., *Handbook of Mathematical Functions with Formulas, Graphs and Mathematical Tables*. New York: Dover, 1977, p. 17.

A Multiresolution Method for Simulating Infinite Periodic Arrays

Dejan S. Filipović, Lars S. Anderson, and John L. Volakis

***Abstract*—Hierarchical mixed-order tangential vector finite elements (TVFEs) for tetrahedra are attractive for accurate and efficient analysis of a wide class of electromagnetic radiation and scattering problems. They provide versatile geometrical modeling and accurate field representation by allowing combination of lowest and higher order TVFEs. In this letter, the finite-element boundary-integral (FE–BI) method with hierarchical TVFEs for tetrahedra is used for analysis of infinite, doubly periodic antenna arrays. It is shown that accurate prediction of array scanning properties can be obtained by using higher order TVFEs in the regions where large fields and rapid field variations are expected and lowest order TVFEs elsewhere. This is demonstrated in the case of a microstrip patch array.**

***Index Terms*—Antenna arrays, finite-element methods, periodic structures.**

I. INTRODUCTION

The infinite array model accurately predicts the scanning properties of the vast majority of antenna elements within a large finite phased array. Applying Floquet's theorem [1] and the appropriate boundary conditions, the infinite array geometry can be reduced to a single periodic cell, referred to as a unit cell. This significantly reduces the computational domain and an appropriate full wave method can then be used for array simulation. In the past, mode matching and the spectral domain method of moments (MoM) have been used, but for better modeling of the feed structure and/or volumetric inhomogeneities within the unit cell, techniques such as the hybrid MoM or finite-element methods (FEMs) are more attractive.

Pozar and Schaubert [2] applied the spectral domain MoM to simulate the scanning properties of infinite periodic arrays of microstrip patches, whereas Tsay and Pozar [3] applied a hybrid MoM/Green's function method for modeling printed arrays associated with volumetric inhomogeneities within the grounded substrate of the unit cell. McGrath and Pyati [4] employed the lowest order tetrahedral tangential vector finite elements (TVFEs) for expanding the electric field within the unit cell in conjunction with a Floquet modal expansion. Lucas and Fontana [5] used a similar approach but applied second order tetrahedral TVFEs. Eibert *et al.* [6] applied the finite-element boundary-integral (FE–BI) method with prismatic TVFEs and the free-space infinite periodic Green's function to simulate a wide class of complex periodic geometries.

In this letter, we apply multiresolution field modeling within a hybrid FE–BI formulation for simulating infinite, doubly periodic antenna arrays. We use the hierarchical mixed-order tetrahedral TVFEs recently introduced by Andersen and Volakis [7] to obtain a computational model that accurately predicts the overall array behavior. Since the properties of hierarchical TVFEs allow for simultaneous use of lowest and higher order TVFEs within the same computational domain, we use higher order TVFEs only within and near the regions associated with highly varying field intensities. The lowest order TVFEs are employed elsewhere to achieve an accurate and efficient field modeling. We show that combining mixed-order TVFEs allows for much coarser

Manuscript received August 2, 1999; revised June 2, 2000.

The authors are with the Radiation Laboratory, Department of Electrical Engineering and Computer Science, The University of Michigan, Ann Arbor, MI 48109-2122 USA (e-mail: {dejan; andersen; volakis}@umich.edu).

Publisher Item Identifier S 0018-926X(00)10839-7.

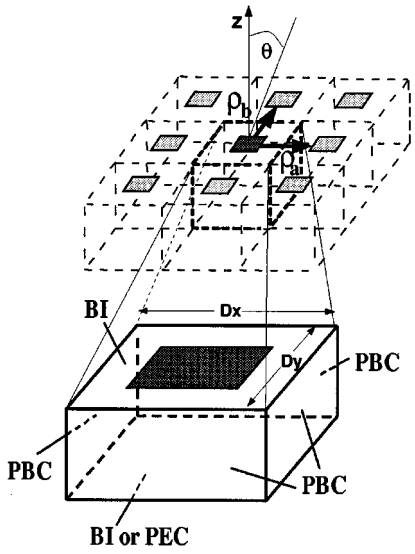

Fig. 1. Geometry of an infinite, 3-D doubly periodic antenna array.

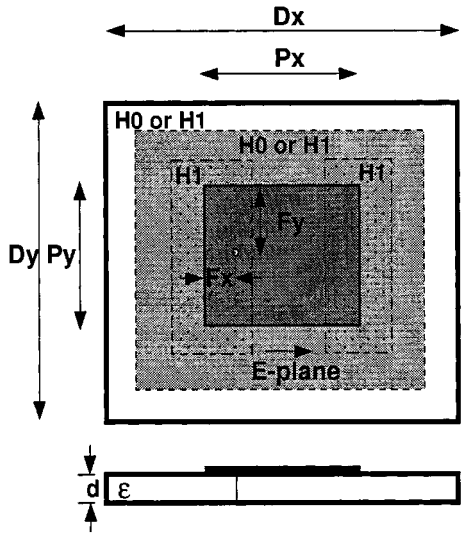

Fig. 2. Infinite periodic microstrip patch array: $(Dx, Dy, Px, Py, Fx, Fy, d) = (5, 5, 3, 3, 0.75, 1.5, 0.2)$ cm, $\epsilon = 2.55$.

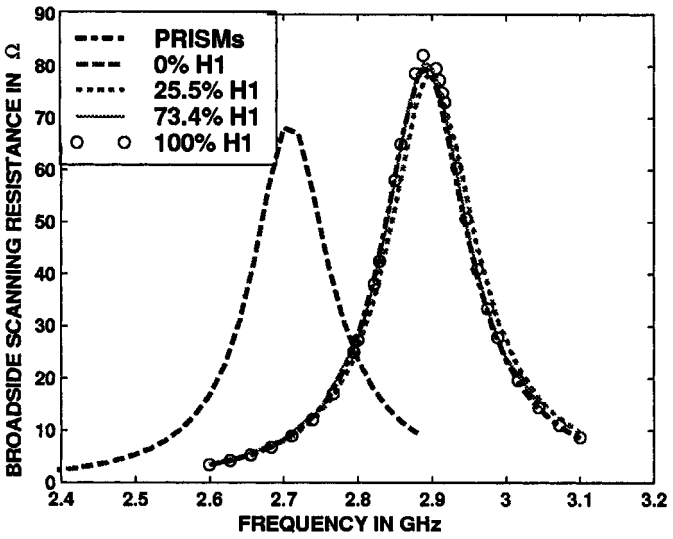

(a)

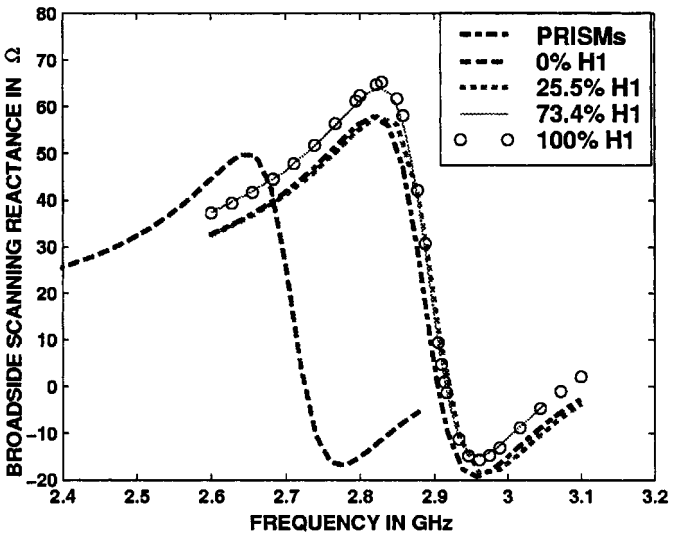

(b)

Fig. 3. Broadside scanning input (a) resistance, and (b) reactance for the infinite patch array whose unit cell is given in Fig. 2.

discretizations as compared to using only the lowest order TVFEs. As a result, the number of unknowns and CPU time are substantially reduced. To demonstrate the effectiveness of the hierarchical TVFEs, we simulate a microstrip patch array and give comparisons with more traditional implementations based on the lowest order tetrahedral and prismatic TVFEs.

II. Formulation

Consider an infinite, doubly periodic printed antenna array on a multilayered, possibly inhomogeneous substrate, as depicted in Fig. 1. We decompose the infinite periodic array structure down to a single unit cell and employ the FEM with the appropriate periodic boundary conditions (PBCs) at the side walls to model the unit cell volume [4], [6]. To truncate the finite element mesh on the top and/or bottom of the unit cell aperture, a BI method is applied in conjunction with the free space infinite periodic Green's function whose computation is accelerated by Ewald's transformation [6]. It is important to note that use of the FEM for modeling the substrate material inherently provides the freedom to analyze various inhomogeneities within the substrate.

Choosing hierarchical mixed-order tetrahedral TVFEs for volume tessellation [7], the electric field within the computational domain can be expanded using six vector basis functions per mixed-order tetrahedral TVFE of order 0.5 (H0 TVFE) and 20 vector basis functions per mixed-order tetrahedral TVFE of order 1.5 (H1 TVFE). In this manner, regions expected to have rapid field variations can be modeled using higher order TVFEs, whereas regions with slowly varying fields can be modeled using lower order TVFEs. Use of various polynomial orders for field expansion within the same computational domain (unit cell) forms the basis of our multiresolution modeling approach. Note, however, that the term multiresolution is not associated with wavelet type basis functions.

Since the edge-based vector basis functions for the H0 TVFE reduce to the Rao–Wilton–Glisson vector basis functions [8] on the unit cell aperture, the latter elements are natural for representing the aperture field in conjunction with the infinite periodic free space Green's function. To close the computational domain, PBCs are imposed on the vertical side faces of the unit cell through the matrix element transformation algorithm [4]. However, this algorithm is generalized to include the case where H1 TVFEs bound the vertical side faces of the unit cell.

We note that when lowest and higher order TVFEs are used in a multiresolution fashion, faces and edges at any boundary between them are treated using the lowest order expansion to preserve continuity of the tangential component of the electric field.

III. Results

Let us consider the microstrip patch array shown in Fig. 2. Our aim is to use this geometry for demonstrating the effectiveness of the proposed multiresolution modeling approach. The input impedance at broadside is computed using various TVFEs and discretizations: 1) prismatic TVFEs [9] with $\lambda_0/40$ sampling and 2744 unknowns; 2) tetrahedral H0 TVFEs with 2544 unknowns; 3) tetrahedral H0/H1 TVFEs with 25.5% H1 TVFEs in the unit cell and 4822 unknowns; 4) tetrahedral H0/H1 TVFEs with 73.4% H1 TVFEs in the unit cell and 10 360 unknowns; 5) tetrahedral H1 TVFEs and 13 127 unknowns. When employing tetrahedral tessellation, the sampling is approximately $\lambda_0/28$ and tetrahedral elements are obtained by splitting each prism into three tetrahedra. H1 TVFEs are placed around the radiating edges as shown in Fig. 2 to improve the field modeling in the vicinity of these regions where the field is expected to be highly varying.

As seen from Fig. 3, the multiresolution expansion generates significantly more accurate results for the input impedance as compared to using only the lowest order TVFEs. Results associated with using H1 TVFEs within 25.5%, 73.4%, and 100% of the unit cell region are almost identical and agree very well with those based on prismatic TVFEs. From Fig. 3, we also observe that the computed input impedance and broadside resonant frequency cannot be accurately determined when nominal sampling is used unless higher order TVFEs are employed (the broadside resonant frequency calculated using MoM is 3 GHz [2]). Basically, when using only the lowest order TVFEs, the mesh has to be significantly denser to give comparable accuracy. Of importance is also that higher order TVFEs can be introduced without retessellation and at any arbitrary location without concerns of element to element discontinuities. However, it is important to note that use of higher order TVFEs should be kept to a minimum, not only for reducing the number of unknowns, but also to keep the matrix condition number as small as possible. We note that the corresponding E-plane and H-plane scanning reflection coefficients agree very well with MoM [2] data and data based on prismatic TVFEs, provided a certain percentage of higher order TVFEs are introduced.

IV. Conclusion

In this letter, we introduced a multiresolution hybrid FE–BI method for modeling infinite doubly periodic antenna arrays. We showed that by using hierarchical mixed-order tetrahedral TVFEs and combining lowest and higher order TVFEs within the computational domain, the accuracy of the field modeling is dramatically improved and the array scanning properties are therefore more accurately evaluated. Higher order TVFEs were used only within those regions where large fields and/or rapid field variations occurred, whereas lowest order TVFEs were used elsewhere. This allowed for the use of coarse meshes and led to significant CPU time and memory savings.

References

[1] *Theory and Analysis of Phased Array Antenna*, Bell Telephone Lab., 1972.

[2] D. M. Pozar and D. H. Schaubert, "Analysis of an infinite array of rectangular microstrip patches with idealized probe feeds," *IEEE Trans. Antennas Propagat.*, vol. AP-32, pp. 1101–1107, Oct. 1984.

[3] W-J. Tsay and D. M. Pozar, "Radiation and scattering from infinite periodic printed antennas with inhomogeneous media," *IEEE Trans. Antennas Propagat.*, vol. 46, pp. 1641–1650, Nov. 1998.

[4] D. T. McGrath and V. P. Pyati, "Periodic structure analysis using hybrid finite element methods," *Radio Sci.*, vol. 31, pp. 1173–1179, Sept./Oct. 1996.

[5] E. W. Lucas and T. W. Fontana, "A 3-D hybrid finite element/boundary element method for the unified radiation and scattering analysis of general infinite periodic arrays," *IEEE Trans. Antennas Propagat.*, vol. AP-43, pp. 145–153, Feb. 1995.

[6] T. F. Eibert, J. L. Volakis, D. R. Wilton, and D. R. Jackson, "Hybrid FE/BI modeling of 3D doubly periodic structures utilizing triangular prismatic elements and MPIE formulation accelerated by the Ewald transformation," *IEEE Trans. Antennas Propagat.*, vol. 47, pp. 843–850, May 1999.

[7] L. S. Andersen and J. L. Volakis, "Hierarchical tangential vector finite elements for tetrahedra," *IEEE Microwave Guided Wave Lett.*, vol. 8, pp. 127–129, Mar. 1998.

[8] S. M. Rao, D. R. Wilton, and A. W. Glisson, "Electromagnetic scattering by surfaces of arbitrary shape," *IEEE Trans. Antennas Propagat.*, vol. AP-30, pp. 409–418, May 1982.

[9] T. Özdemir and J. L. Volakis, "Triangular prisms for edge-based vector finite element analysis of conformal antennas," *IEEE Trans. Antennas Propagat.*, vol. 45, pp. 788–797, Apr. 1997.